Conjunctive use of floodwater harvesting for managed aquifer recharge and irrigation on a date farm in Morocco

Yassine Khardi, Guillaume Lacombe, Benoît Dewandel, Ali Hammani, Abdelilah Taky, Sami Bouarfa

Received: 25 August 2023 | Revised: 27 March 2024 | Accepted: 27 March 2024

DOI: 10.1002/ird.2967

RESEARCH ARTICLE

WILEY

Conjunctive use of floodwater harvesting for managed aquifer recharge and irrigation on a date farm in Morocco

Yassine Khardi[1,2,3] | **Guillaume Lacombe**[1,2] | **Benoit Dewandel**[4] | **Ali Hammani**[1] | **Abdelilah Taky**[1] | **Sami Bouarfa**[5]

[1]Hassan II Agronomic and Veterinary Institute, Rabat, Morocco

[2]CIRAD, UMR G-EAU, Montpellier, France

[3]L'institut Agro Montpellier, Montpellier, France

[4]BRGM Occitanie region, UMR G-EAU, Montpellier, France

[5]INRAE Occitanie-Montpellier, UMR G-EAU, Montpellier, France

Correspondence
Guilaume Lacombe, CIRAD, UMR G-EAU, 34398 Montpellier, France.
Email: guillaume.lacombe@cirad.fr

Funding information
International Fund for Agricultural Development, Grant/Award Number: 2000002013

Abstract

In arid regions, harvesting floodwater can mitigate irrigation-induced groundwater depletion by providing additional surface water and recharging aquifers. We designed an experimental protocol to quantify these fluxes on a date farm located along the Wadi Satt, whose flow originates from the Anti-Atlas Mountains in south-eastern Morocco. Automatic barometric sensors were used to monitor the water level in a 6500 m^3 floodwater harvesting pond and in surrounding boreholes. Six flood events occurred from 2021 to 2023. The pond water balance indicated that most stored water is pumped for irrigation (56% of harvested floodwater). More than 40% infiltrates at a rate of approximately 90 mm day^{-1}, and the remainder evaporated. Analytical modelling of the pond water table system showed that the radius of the piezometric mound resulting from pond infiltration is less than 360 m. Groundwater recharge from the irrigated plot could be observed after two close floods that enabled continuous pumping for several weeks, suggesting that in this specific context, over-irrigation using surface water allows the aquifer to be recharged. The hydrological effects of possible future expansion of these ponds at the watershed scale should be analysed to assess possible negative impacts on downstream water resources.

KEYWORDS

analytical modelling, floodwater harvesting pond, groundwater recharge, Moroccan oasis, spate irrigation, water balance assessment

Résumé

Dans les régions arides, le captage des eaux de crues peut atténuer l'épuisement des eaux souterraines induite par l'irrigation en fournissant des eaux de surface supplémentaires et en rechargeant les aquifères. Nous avons conçu un protocole expérimental pour quantifier ces flux sur une ferme de palmiers

Article title in French: Utilisation conjuguée des eaux de crues pour la recharge de la nappe et l'irrigation du palmier dattier à l'échelle de l'exploitation agricole au Maroc.

dattiers située le long de l'oued Satt, dont les écoulements proviennent de l'Anti-Atlas au sud-est du Maroc. Des sondes barométriques automatiques à enregistrement continu ont été utilisées pour suivre le niveau d'eau dans un bassin de collecte des eaux de crues de 6500 m^3 et dans les forages environnants. Six crues se sont produites de 2021 à 2023. Le bilan hydrique du bassin indique que la plus grande partie de l'eau stockée est pompée pour l'irrigation (56% des eaux de crues captées). Plus de 40% s'infiltrent à un taux d'environ 90 mm $jour^{-1}$, et le reste s'évapore. La modélisation analytique de la recharge de la nappe a montré que le rayon du dôme piézométrique résultant de l'infiltration de l'eau stockée dans le bassin est inférieur à 360 mètres. La recharge de la nappe sous la parcelle irriguée a été observée suite à deux crues successives ayant permis un pompage dans le bassin de stockage et une irrigation continue pendant quelques semaines, révélant le rôle complémentaire de la sur-irrigation dans ce dispositif de recharge. Les effets hydrologiques d'une éventuelle multiplication de ces bassins de recharge à l'échelle du bassin versant devraient être analysés afin d'évaluer les effets négatifs possibles sur les ressources en eau à l'aval.

MOTS CLÉS

irrigation par les eaux de crue, recharge des aquifères, bassin de récolte des eaux de crue, évaluation du bilan hydrique, modélisation analytique, oasis marocaine

1 | INTRODUCTION

Dryland agriculture relies on many ancestral irrigation and rainwater-catching practices. In Morocco, a range of these practices are used, including 'Matfia', 'Jessours', 'Tabia' and 'Meskat' (El Yadari et al., 2019; Koutous et al., 2023; Sabir et al., 2010). These hydraulic structures are increasingly being replaced by collinear dams and large cisterns (Prinz, 1996). In Moroccan oases, *khettaras* and spate irrigation are good examples of such practices (Faiz & Ruf, 2010; Lightfoot, 1996). Since the 1980s, these collective and sustainable irrigation practices have progressively been replaced by individual irrigation systems that rely on wells and boreholes equipped with pumps powered by diesel fuel or gas and, more recently, solar energy (Dione, 2012). This rapid expansion is exerting growing pressure on increasingly scarce groundwater resources (Khardi et al., 2023), but some farmers are replicating collective practices at the individual level. For example, wadi floodwater is harvested in earthen farm ponds to increase the supply of irrigation water and to locally recharge the aquifer (Khardi et al., 2024).

Msume et al. (2022) inventoried several floodwater-based irrigation systems: flood recession agriculture, depression agriculture, spate irrigation, and inundation canals and dugouts. The diffusion and adoption of these practices in rural areas depend on affordability and farmers' awareness, entrepreneurship and capital (Msume et al., 2022). Godwin et al. (2022) evaluated the feasibility of using farm-level infiltration galleries to recharge groundwater. Arshad et al. (2014) developed a method to evaluate the financial feasibility of managed groundwater recharge, and in India, Soni et al. (2020) evaluated the performance of farm recharge wells and their impact on the quality of drinking water and the possibility of increasing the supply of irrigation water.

A variety of methods are available for quantifying groundwater recharge, including lysimeter measurements (Gee & Hillel, 1988; Xu & Chen, 2005), surface and/or groundwater balance measurements (Boisson et al., 2014; Kendy et al., 2003; Maréchal et al., 2006), estimations via natural tracers (Wang et al., 2008; Zhu, 2000) and inverse modelling (Hashemi et al., 2013).

One of the best known and most frequently cited methods for evaluating groundwater recharge is the analytical solution provided by Hantush (1967), which has been extensively evaluated and compared with numerical modelling. Many authors (e.g. Carleton, 2010; Warner et al., 1989) have demonstrated its high level of accuracy in evaluating the growth and decay of groundwater mounds below infiltration ponds (Finnemore, 1995; Zomorodi, 2012).

As described by Khardi et al. (2024), the purpose of harvesting floodwater using a farm pond may be

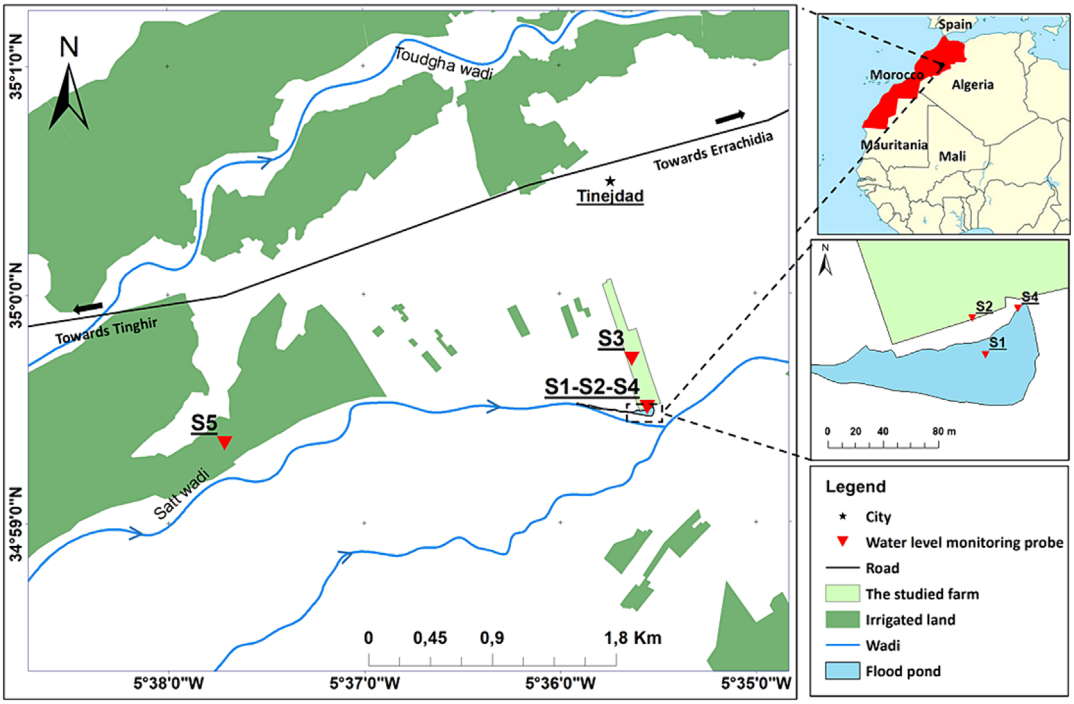

FIGURE 1 Location of the farm and groundwater monitoring probes.

twofold: (i) recharging groundwater and (ii) supplying water for surface irrigation. However, the two objectives may conflict. Recharging groundwater from a pond requires conditions that favour infiltration, whereas providing water for surface irrigation requires minimizing infiltration and maximizing direct pumping from the pond. The aim of our study was to understand the potential complementarities between these two purposes, that is, direct pumping from the pond for surface irrigation and groundwater recharge. To this end, we combined experimentation and modelling. Water balances were derived from on-site measurements of surface and groundwater levels combined with farmer interviews to understand irrigation practices. Analytical modelling was performed to verify whether infiltration rates assessed from the pond water balance could explain the piezometric variations in the water table, thus revealing groundwater recharge.

2 | MATERIALS AND METHODS

2.1 | Study area

The farm we studied is located in the Drâa-Tafilalet region of Morocco along the Wadi Satt, which has its source in the Anti-Atlas Mountains. The irrigation water used on the farm originates from wadi floods and groundwater (Figure 1). Wadi flows intermittently in the form of flash floods produced by rare but intense rainfall events. The Satt watershed area upstream of the farm extends more than approximately 790 km^2. The average annual rainfall is approximately 140 mm, with a standard deviation of approximately 70 mm (Station Ait Bouijane 1961–2018). As for the majority of farms in the region, water pumped from the Quaternary alluvium and underlying fractured schist–quartzite aquifers is the main permanent source of irrigation water. The farm studied has two separate irrigation systems relying on groundwater and floodwater. Groundwater is pumped by solar energy, stored in a geomembrane pond, pumped into a filter and pressurized to irrigate date palms by drip irrigation. Nearby, another 6500 m^3 earthen pond (Figure 2) stores part of the floodwater diverted from the wadi. The average storage area is 3250 m^2, and the average depth is 2 m. The floodwater stored in the pond is pumped into a buried pipe system equipped with five outlets on the ground surface. All of these plants can be irrigated by gravity. Just after the pond is filled with floodwater, the farmer irrigates with floodwater exclusively, stopping drip irrigation from groundwater. An old hand-dug artisanal well located inside the pond was dug before the ponds' banks were built, and some palm trees were planted in the middle of the pond.

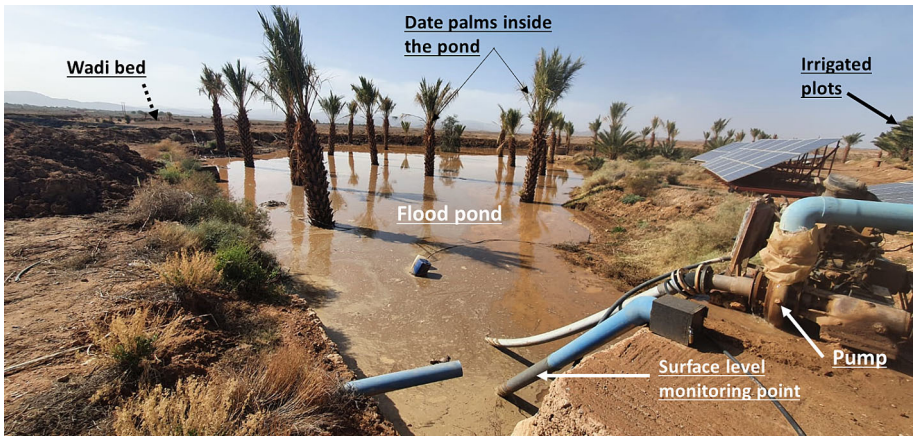

FIGURE 2 The floodwater harvest pond and the pump intake 1 day after the flood that occurred on 9 March 2021.

2.2 | Methods

2.2.1 | Monitoring devices and field measurements

An experimental protocol was established to evaluate the volumes of floodwater stored in the pond used either directly to feed the irrigation system through pumping or to recharge the water table. Water levels were monitored with automatic barometric sensors installed in a 12-m deep well located inside the pond itself (S1); in two boreholes located approximately 30 and 360 m from the pond (S2 and S3); in the pond (S4); and in a well located approximately 3 km upstream of the farm and 180 m away from the wadi (S5) (Figure 1). Two boreholes, S2 and S3 (depth >80 m), were used to monitor the water levels in the Ordovician quartzite and the shale aquifers. S5 is far enough away not to be influenced by pond recharge but rather to observe the effect of natural recharge from the wadi (Figure 1). To estimate variations in the water level in the absence of bias, an additional sensor was left in the open air to measure the atmospheric pressure, which was subsequently subtracted from the pressure measured underwater. All the sensors were set to record the absolute pressure at 10-min intervals. The depth of the sensors in the wells and boreholes was kept stable by means of fixed-length cables linked to the ground surface. Measurements were taken manually at different water level depths to validate the automatic measurements. The coordinates (x, y, z) of the measurement points were obtained from a topographic survey, and the groundwater levels measured in boreholes S1, S2, S3 and S5 were converted to piezometric levels (i.e. metres above sea level). Floods 4 and 6 were not recorded because sensors S3 and S4 were out of order. Therefore, four floods out of the six that occurred over the 2 years were fully studied; we did not conduct any modelling for flood number 4 (see Figure 5) due to the lack of water level data for the pond, and we did not model the groundwater level in S3 for flood number 6 (Figure 5).

The volume and surface area of the pond were assessed through a topographic survey that included 117 points located at the bottom of the pond and on its banks. The coordinates (x, y, z) of the sampled points were processed in GIS software to obtain the relationships between the height, volume and surface area. Daily rainfall and evapotranspiration data (ET_0), estimated using the Penman–Monteith method, were obtained from the nearest meteorological station located at Goulmima, 23 km to the north (31.68312; 4.95869).

2.2.2 | Pond water balance

The pond water balance accounts for both infiltration and the pumped water volume. Its equation (Equation 1) is solved for periods with no rainfall and no inflow from the wadi. Such conditions prevail most of the year, as the region has an arid climate. The destocking flows from Equation (1) are shown in Figure 3.

$$\Delta h_{\text{pond}} = I_{\text{total}} + \frac{P}{S} + E + \text{ET}_{\text{palm}} \quad (1)$$

where I_{pond} is the infiltration flow from the bottom of the pond (m), I_{well} is the infiltration flow from the S1 well (m), $I_{\text{total}} = I_{\text{pond}} + I_{\text{well}}$, P is the volume of water pumped from the pond for farm irrigation (m^3), S is the surface area of the water in the pond (m^2), Δh_{pond} is the variation in the level of the S4 water (h) in the pond (m), counted as positive in the case of a decrease, E is the evaporation from the pond (m), ET_{palm} is the evapotranspiration from the palm trees planted in the pond (m).

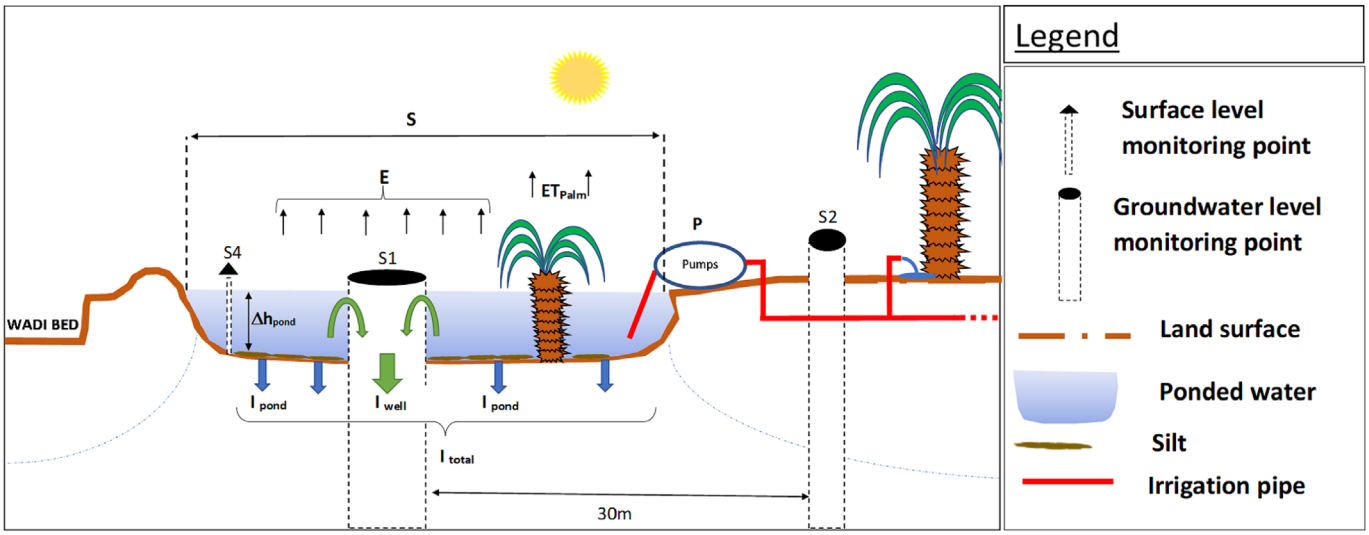

FIGURE 3 Conceptual sketch of the pond, its monitoring devices and destocking flows.

The infiltration rate is determined by solving Equation (1) for different periods of a few hours each, which correspond to contrasting ranges of water levels. These computation periods were selected based on three criteria: (i) the last flood had occurred more than 1 day previously to avoid delayed inflow into the pond, (ii) during the night (i.e. between 6 pm and 6 am) in the absence of pumping, and (iii) when the water level drawdown was almost constant over time. The three conditions were confirmed by checking the pond water level time series (S4) at 10-min intervals. Over these computation periods, Equation (1) simplifies and results in Equation (2):

$$I_{\text{total}} = \Delta h_{\text{basin}} - E - \text{ET}_{\text{palm}} \quad (2)$$

E and ET_{palm} were each approximated by ET_0, likely resulting in overestimation, given that the palm trees in the pond are planted sparsely (i.e. their crop coefficient is lower than unity), while E and ET_0 are comparable (Khardi et al., 2024). According to Equation (2), this overestimation leads to underestimation of I_{total}, indicating that our results are conservative. Nevertheless, this bias is negligible because Δh is one order of magnitude greater than E and ET_{palm} over the computation periods used.

The rates of infiltration into the well located in the pond were computed using Equation (2) applied to S1 (with $\text{ET}_{\text{palm}} = 0$) for water levels lower than those ensuring hydraulic connection with the pond, that is, when the S1 and S4 time series diverged over a destocking period.

The relationship between the pond water level (h) and its total infiltration rate (I_{total}) was modelled using Equation (3):

$$I_{\text{total}} = a \times h + b \quad (3)$$

where parameters a and b were determined by linear regression for each destocking period following a flood. The uncertainty intervals around the infiltration values depend on those of $E + \text{ET}_{\text{palm}}$, which vary between 0 and $2 \times \text{ET}_0$.

Pumped water ($q = P/S$ [in m]) was derived from Equations (1) and (3) and applied over periods (t) with near constant decreases in water level, which usually last several hours during the day. The start and end of these periods were identified from the S4 time series by visualizing break points in the curve slope ($\Delta h/t_{\text{with pumping}} > \Delta h/t_{\text{without pumping}}$). The uncertainty intervals of the estimated q-values were assessed by including—or not including—the transient time of slope changes resulting from system inertia.

he infiltrated and pumped water volumes were estimated by multiplying I_{total} and q, respectively, by the surface area of the corresponding ponded water obtained from the height–volume–surface (HVS) curve of the pond. The uncertainty of the pumped volumes was calculated by adding the uncertainty of the infiltration to the uncertainty of the wet surface area of the pond; notably, the HVS curve is pseudolinearly related to the intervals of the water balance calculations. The wetted area uncertainty for a given water level h in the pond corresponds to the wetted area of $h \pm 1$ cm. The uncertainty in the

pumped volume (i.e. difference between p_{max} and p_{min}) is calculated as follows:

$$q_{max} = (\Delta h - I + \sigma) * S_{max} \quad (4)$$

$$q_{min} = (\Delta h - I_{max} - \sigma) * S_{min} \quad (5)$$

where I_{max} is the overestimated infiltration flow from the bottom of the pond (m), S_{max} is the wetted area in the pond calculated using the HSV curve for a water level of $(h + \sigma)$ (m^2), S_{min} is the wetted area in the pond calculated using the HSV curve for a water level of $(h - \sigma)$ (m^2), $\sigma = 1 \times 10^{-2}$ m.

2.2.3 | Analytical modelling of recharge

The response of the water table to infiltration from the pond and the well was simulated using an analytical model developed by Dewandel et al. (2021) based on the analytical solution of Hantush (1967). The model assumes an infinite and homogeneous aquifer and a rectangular pond whose surface area is equivalent to the mean ponded surface area obtained from the HVS curve and the S4 time series. The model accounts for predetermined parameters and calibrated parameters and considers variable infiltration rates. The predetermined parameters include the dimensions (length and width $[2x_L;2y_L]$) of the rectangular pond (Figure 4), the location and radius of the recharge well, the location of groundwater level measurements relative to the pond, and the thickness of the aquifer, which is 30 m according to the Water Resources Division (1977). This thickness represents the saturated Quaternary alluvium deposit and the top of the fractured Ordovician aquifer. The calibration parameters included both the hydraulic conductivity (K) and the storage coefficient (S) of the aquifer.

The input variables include the infiltration rates of the pond and recharge well ($I_{pond} + I_{well}$ in Equation 1) as a function of time and the quadratic head losses of the recharge well. Based on records of the S5 probe indicating no response of the piezometric data to the wadi floods, groundwater recharge from the wadi was assumed to be negligible in the model. It is important to note that the wetted surface of the pond decreases during the destocking phase, whereas in the model, it remains constant. Consequently, we first evaluated the possible bias caused by the choice of a fixed rectangular pond in the model. A sensitivity analysis was carried out based on the observations of floods 1 and 2 at point S2. First, the length-to-width ratio was varied to assess the impact of changing the shape of the pond (from a square pond to a rectangular one), and the modelled infiltration area was also varied while respecting the principle of mass conservation. For the first analysis, length-to-width ratios of 1, 2 and 3.5 were tested for an average flooded area of 3250 m^2. In the second analysis, areas of 2700, 4680 and 5790 m^2 were tested. The principle of conservation of mass is applied to the instantaneous volume of water infiltrated, which itself is the product of the infiltration area and the instantaneous infiltration rate.

The model was calibrated for all the recorded floods by selecting the parameter values that corresponded to the best visual match between the observed and simulated piezometric levels at point S2. The visual adjustment primarily concerned the rates of increase and

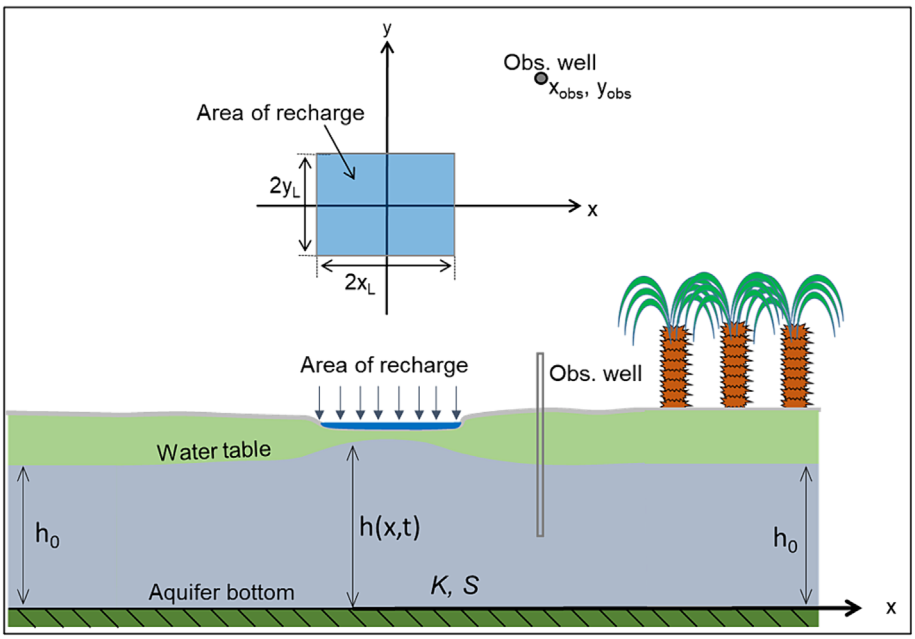

FIGURE 4 Conceptual sketch of groundwater recharge from the pond.

decrease and the maximum filling height. This calibration procedure was repeated at points S3 and S1.

In addition, another version of the model that accounts for the infiltration of floodwater through the wadi bed in the vicinity of the pond was tested to determine the possible influence of natural recharge on water level fluctuations at point S2. Finally, the analytical model used in the present study (Dewandel et al., 2021) included a single pond from which infiltration occurred. Recharge due to return flow from over-irrigation could explain the difference between the observed and modelled recharge from only one pond. Consequently, a trial-and-error method was used to estimate potential irrigation return flows below the root zone, which could explain the piezometric rise observed at point S3. For that purpose, we assumed that the infiltration flow below the root zone only occurred in the irrigated plots and occurred evenly. As several models were tested, only the most significant results are reported here.

2.2.4 | Assessment of water stored in the soil of the irrigated plot

We investigated the possibility of groundwater recharge due to over-irrigation by assessing the water stored in the soil of the entire irrigated zone. Given that infiltration below the root zone depends on both soil and plant parameters, the available water capacity of the soil was approximated based on rooting depth and soil texture (Bruand et al., 2004). The soil texture was obtained from a soil map of the area (ORMVA-Tf, 1987), and the rooting depth of the date palms was estimated following Sedra (2003). The amount of water consumed by date palms every day was obtained from Sabri et al. (2017) and El Khoumsi (2017), whose study areas are located in the Drâa-Tafilalet region. The total amount of water consumed by the date palms was estimated in millimetres from the product of the number of irrigated date palms, the total volume of water consumed by the date palms daily and the inverse of the area irrigated by floodwater. Interviews with the farmers allowed us to understand the irrigation calendar and interpret the variations in the S4 water level decreases, some of which were caused by pumping.

3 | RESULTS AND DISCUSSION

3.1 | Water levels

During and immediately after each of the first four floods, the water levels in the pond (S4) and in the well inside the pond (S1) started to increase in the same way: a sharp increase that lasted for several minutes, followed by a decrease that lasted more than 47 h, after which the two curves separated. A split occurred when the water levels at points S1 and S4 reached 1014.5 m. Below this water level, the level in S1 decreased much faster than that in S4, suggesting that the well was hydraulically disconnected from the pond. Field observations revealed a 3-cm wide crack in the wall of the well at the height corresponding to the split between the S1 and S4 curves, confirming that the recharge function of this old well was accidental. Independent of its connection with the well, the S4 curve exhibited a stair-step pattern caused by the alternation of periods with pumping (the curve of S4 was steeper during the day) and without pumping (the curve of S4 was less steep at night). This pumping aims to irrigate the farm (Figures 3 and 5).

Although the piezometric profile measured in the S2 borehole corresponds to that of all pond fills, the maximum piezometric strength reached during each flood decreased over time. This negative trend likely reflects a similar trend in large-scale piezometry, but it could also be due to the progressive silting of the pond, which reduced the infiltration rate. The last two floods (nos. 5 and 6) were quite brief compared to the previous floods. The piezometric activity in borehole S3 increased simultaneously following floods 1 and 2 only and then, despite subsequent floods and piezometric reactions in S1 and S2, continued to decrease gradually until the records ended.

Drip irrigation has no observable effect on groundwater recharge. In fact, drip irrigation is used throughout the year, but our records of the piezometric level show a reaction from the aquifer only after flooding.

3.2 | Infiltration rates in the pond and recharge flow from the well

The infiltrated flows from the recharge well did not exceed 0.7 $m^3\ h^{-1}$ or 17 $m^3\ day^{-1}$. This flow rate is lower than the infiltration rates in injection and recharge wells around the world, which have recharge capacities ranging from 1700 to 6000 $m^3\ day^{-1}$ (Casanova et al., 2013).

The infiltration rates from the pond fluctuated between 1×10^{-3} and 9×10^{-3} $m\ h^{-1}$ (Appendix A). When the maximum surface area of the pond (6400 m^2) was taken into account, the rate exceeded 100 $m^3\ day^{-1}$. Thus, only infiltration from the pond (excluding that from the well) was considered in the following calculations.

According to Dillon et al. (2019) and Wuilleumier and Seguin (2008), typical infiltration rates for recharge

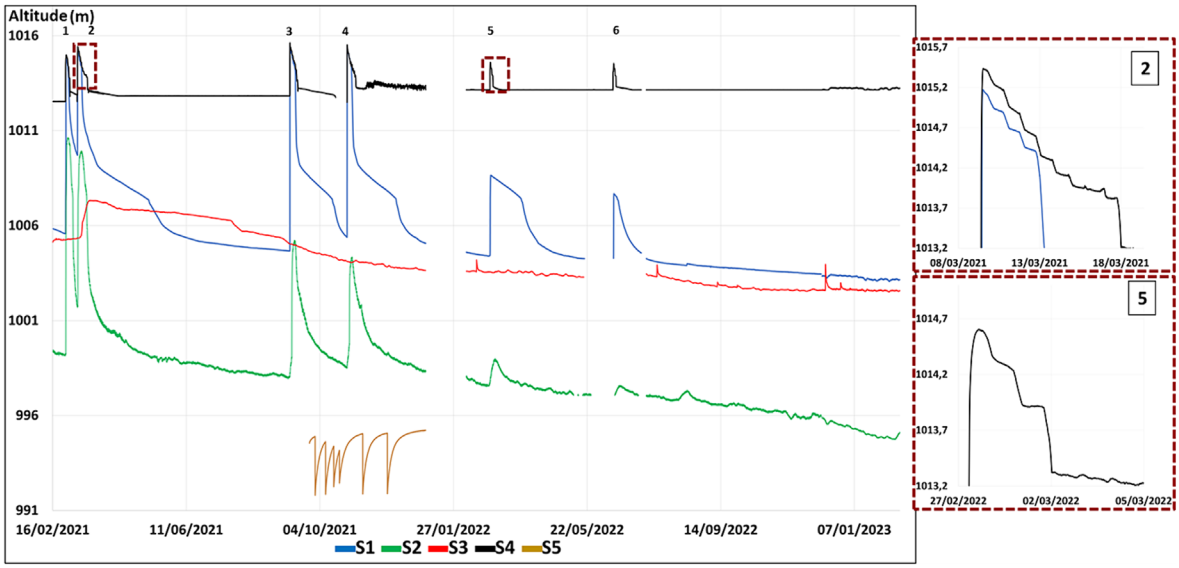

FIGURE 5 Graph of the water level in the pond and in the piezometers installed to monitor the groundwater level.

ponds fluctuate between 0.3 and 1 m day^{-1}. The highest rate of the pond used in the present study (<0.21 m day^{-1}) exhibited very low performance. This suboptimality can be explained by the fact that the location of the pond was determined by land access constraints rather than by geological conditions.

Figure A1 shows that, for a given flood, the rate of infiltration is positively correlated with the level of water in the pond, suggesting that a hydraulic process follows Darcy's law. Accordingly, for a given water level, the infiltration rate tends to decrease over successive floods in response to the silting of the pond. The recurrent removal of silt (which is used to fertilize the soil in the palm grove) could explain the irregularities we observed in this trend.

3.3 | Pond water balance

Figure 6 shows that evaporation and evapotranspiration represented less than 3.8% of the floodwater harvested over the study period. The infiltration volumes in Figure 6 were obtained by including the infiltration rates reported in Appendix A. The ratio of the infiltrated to pumped volume of water per flood event tended to decrease over time, from 1 : 1 for the first flood to 1 : 3 for the last one (Figure 6). This decrease was probably due to two factors: (i) less water infiltrated due to silting, and more water was pumped to irrigate the date palms; (ii) the total volume of harvested floodwater decreased over successive floods from 4724 m^3 for the first flood to 2473 m^3 for the last flood. Thus, the correspondingly lower water levels in the pond reduced the rate of infiltration. Maximizing irrigation when infiltration diminishes helps reduce the loss of water from the pond due to evaporation.

3.4 | Analytical modelling of groundwater level

For our specific case study, analytical modelling was used to understand the response of a complex and insufficiently documented aquifer. The application of this universal method on a local scale, particularly on a farm, is useful.

Regarding the sensitivity test related to the choice of a fixed rectangular pond area for the purpose of modelling, we deduced that the errors linked to this choice are less important than other errors not taken into account by the model (e.g. estimating infiltration rate, silting and the heterogeneity of the aquifer). On the one hand, the model was recalibrated by increasing the storage coefficient parameter by approximately 40% while maintaining the same hydraulic conductivity for floods 1 and 2 for the same length/width ratio variation. On the other hand, almost no changes in hydraulic conductivity or storage coefficient were needed in the sensitivity analysis for ponds with varying surface areas in the 2700 and 4680 m^2 areas. To calibrate the model to an area of 5790 m^2, we reduced the storage coefficient by 20%.

Figure 7 shows the observed and simulated groundwater levels at point S2. All the pond fills led to an increase in the observed and modelled water levels. The values of hydraulic conductivity $K = 4.1 \times 10^{-6}$ m s^{-1} and storage coefficient $S = 3.5 \times 10^{-3}$ led to the best

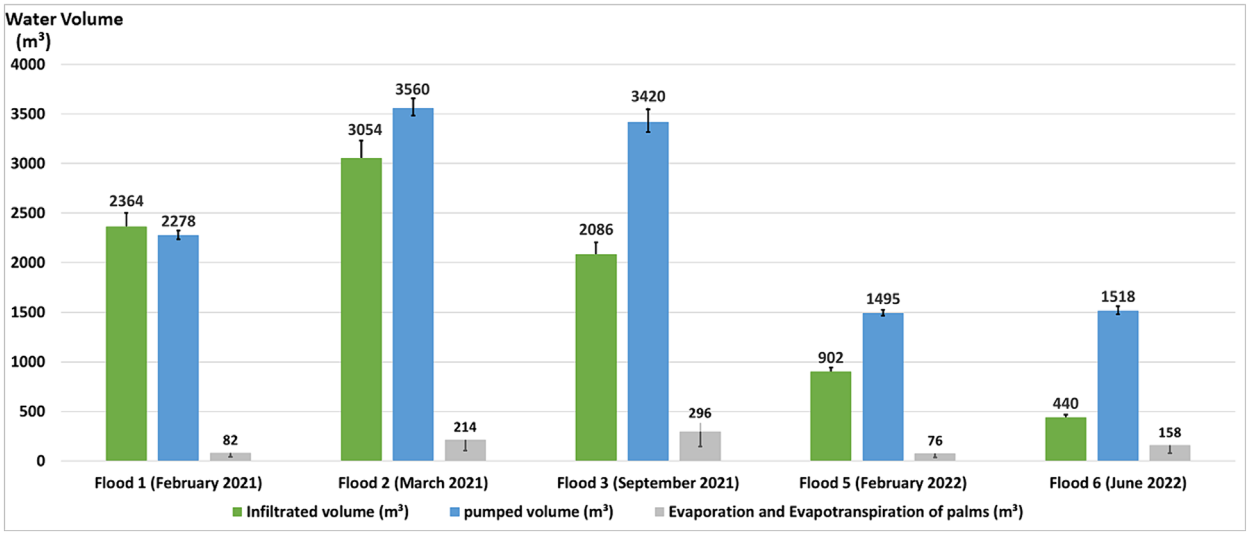

FIGURE 6 Water balances (in m^3) for the recorded floods.

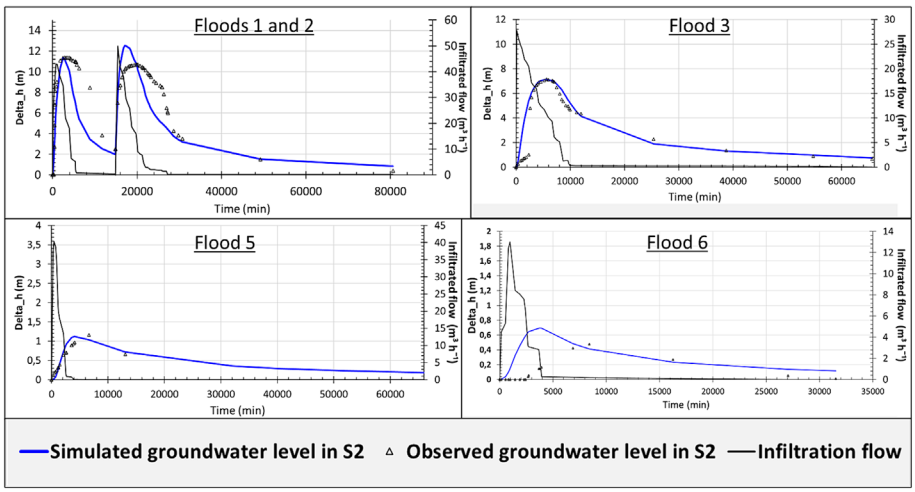

FIGURE 7 Modelling of groundwater recharge in S2.

match between the observed and simulated values for the first and second floods (in which we assumed a model infiltration area equivalent to the average area of the real pond). These values are typical of unconfined fractured aquifers (Dewandel et al., 2006; Lachassagne et al., 2021).

The third, fifth and sixth floods were modelled and fitted using the values of hydraulic conductivity and storage coefficient $K = 2.2 \times 10^{-6}$ m s^{-1}, $S = 8.5 \times 10^{-3}$; $K = 3 \times 10^{-6}$ m s^{-1}; $S = 5 \times 10^{-2}$; and $K = 5 \times 10^{-6}$ m s^{-1}, $S = 3 \times 10^{-2}$, respectively. Floods occurred at increasingly deeper piezometric levels, and the aquifer took longer to respond to the inflow of water resulting from infiltration (Figure 5). Since the model does not account for the depth of the water table (infiltration is assumed to reach the saturated aquifer directly), we needed to increase the storage coefficient and/or reduce the modelling hydraulic conductivity to account for the delayed response of the water table.

The K and S-values reveal a general decrease in diffusivity ($\nu = T/S$; $T = BK$ with B: aquifer thickness) of the modelled aquifer. In this context, the hydraulic conductivity values remain coherent, but the storage coefficients are apparent values. In other words, the system takes more time to react to infiltration from the pond, which is modelled while decreasing ν. This delay can be explained by the fact that the aquifer is deeper and the unsaturated zone is consequently thicker. This could also be explained by the fact that aquifer fracturing decreases with depth and that part of the infiltrated water is not intercepted in S2 (Guihéneuf et al., 2014).

TABLE 1 Water supply and demand by date palm for irrigation and potential return flow to groundwater.

Event	Flood irrigation period (day)	Water supplied to the soil by irrigation (mm)	Water consumed by the date palms (mm)	Potential return flow (mm)
Flood 1 (27 February 2021)	3	31	7	24
Flood 2 (9 March 2021)	8	49	27	22
Flood 3 (8 September 2021)	6	47	30	17
Flood 5 (27 February 2022)	3	21	7	14
Flood 6 (13 June 2022)	3	21	19	2

At the start of the third and sixth flood events, we observed a marked difference between the observed and simulated groundwater levels. This difference may be due to the estimated rate of infiltration (due to silting of the bottom of the pond).

In the first and second floods, we observed a difference between the observed and simulated groundwater levels during the emptying of the pond (from $t = 4000$ min to $t = 14{,}000$ min and from $t = 20{,}000$ to $t = 30{,}000$ min, respectively, for the first and second floods). This difference can be explained by the delayed drainage of the unsaturated zone due to irrigation, which reaches the groundwater later and contributes to its recharge.

As mentioned above, other modelling approaches were used (data not shown), and the results showed that considering the irrigation return flow from the irrigated plots simultaneously with infiltration from the pond could explain the difference between the modelled and observed results. Finally, the model in which a wadi was located next to the pond confirmed that the effect of infiltration from the wadi on the fluctuations at S2 was very small.

At point S3, the same hydraulic conductivity and storage coefficient values obtained from the calibration of S2 were applied by assuming that the structure of the aquifer was homogeneous. However, the model was unable to reproduce fluctuations in the water level resembling those observed in S3. Other hydraulic conductivity and storage coefficient values were tested but in vain. Additionally, the fluctuations observed at point S3 were not related to the filling and emptying cycles of the pond (Figure 5). Hence, a hydraulic disconnection between points S2 and S3 can be inferred. A model with a no-flow boundary was tested, and the results were confirmed (data not shown). Over-irrigation may cause a return flow of irrigation water to the aquifer near point S3, which may explain the piezometric response after the second flood. Thus, given the hydraulic disconnection, the irrigation return flow at point S3 can be modelled without considering infiltration from the pond.

3.5 | Assessment of water in the soil of the irrigated plot

Based on an average rooting depth of 1–1.5 m and an available water capacity of 1.5 mm cm^{-1}, the soil water capacity of the palm grove was estimated to be greater than 150 mm. The quantity of water consumed by the date palms daily is 2.2, 4.5 and 6.4 mm for the months of February, September and June, respectively (El Khoumsi, 2017). Table 1 summarizes the average water supply by irrigation and the consumption of date palms during flood irrigation episodes.

The trial-and-error method applied to the entire irrigated area showed that an infiltration flux between 2 and 3 mm day^{-1} spread over a period of 8 days from the beginning of the second flood could generate a response in the water table similar to that observed at point S3 after the second flood. Table 1 shows that such a rate could only have occurred during the first two floods. In particular, during these first two floods, a difference between the observations and the model based on infiltration from the pond was observed only when the pond was emptied.

4 | CONCLUSION

The multiplication of wells and boreholes over recent decades in the Draa-Tafilalet region and the consecutive drawdown of piezometric levels have incentivized farmers to revert to surface water collection for their irrigation needs. From this perspective, managed groundwater recharge aims to store flash floodwater that would be lost by evaporation in this arid environment.

Our results have shown that the efficiency of recharging groundwater with harvested flood water is greatly constrained by the heterogeneity of the aquifer combined with land availability for the recharge pond.

However, locally deployed irrigation practices can overcome these constraints. As the pond siltation reduces both its storage capacity and permeability, more of the

stored water is pumped for irrigation. This practice both mitigates any potential increase in evaporation and, in the case of successive floods enabling prolonged pumping from the pond, contributes to groundwater recharge through over-irrigation.

Although this study demonstrated the benefits of floodwater harvesting for groundwater recharge in the Drâa-Tafilalet region, it highlighted a constraint: recharged groundwater may circulate outside of the areas where its promoter is allowed to drill and pump. While such an impediment could be anticipated by local hydrogeological investigations, adopting a different paradigm considering that recharged water is potentially beneficial to a larger community at a wider geographic scale could solve this issue. Acknowledging this, public institutions could promote collectively managed groundwater recharge projects likely to benefit a region rather than specific individuals. However, regionalizing managed groundwater recharge could significantly reduce floodwater reaching downstream users, thus calling for a water management plan at the watershed level.

DATA AVAILABILITY STATEMENT

The data that support the findings of this study are available from the corresponding author upon reasonablerequest.

ORCID

Yassine Khardi https://orcid.org/0000-0002-0648-8612

REFERENCES

Arshad, M., Guillaume, J.H.A. & Ross, A. (2014) Assessing the feasibility of managed aquifer recharge for irrigation under uncertainty. *Water*, 6(9), 2748–2769. Available from: https://doi.org/10.3390/w6092748

Boisson, A., Baïsset, M., Alazard, M., Perrin, J., Villesseche, D., Dewandel, B. et al. (2014) Comparison of surface and groundwater balance approaches in the evaluation of managed aquifer recharge structures: case of a percolation tank in a crystalline aquifer in India. *Journal of Hydrology*, 519, 1620–1633. Available from: https://doi.org/10.1016/j.jhydrol.2014.09.022

Bruand, A., Duval, O. & Cousin, I. (2004) *Estimation des propriétés de rétention en eau des sols à partir de la base de données SOL-HYDRO: Une première proposition combianant le type d'horizon, sa texture et sa densité apparente*. Sols: Étude Gest.

Carleton, G.B. (2010) Simulation of groundwater mounding beneath hypothetical stormwater infiltration basins. US Geol. Surv. Sci. Inv. Rep. 2010–5102, 64 pp. Available from: https://doi.org/10.3133/sir20105102

Casanova, J., Cagnimel, M., Devau, N. & Pettenati, M. (2013) *Recharge artificielle des eaux souterraines: état de l'art et perspectives*. 227. ONEMA-BRGM, Orléans, France.

Dewandel, B., Lachassagne, P., Wyns, R., Maréchal, J.C. & Krishnamurthy, N.S. (2006) A generalized 3-D geological and hydrogeological conceptual model of granite aquifers controlled by single or multiphase weathering. *Journal of Hydrology, Hydro-Ecological Functioning of the Pang and Lambourn Catchments, UK*, 330(1-2), 260–284. Available from: https://doi.org/10.1016/j.jhydrol.2006.03.026

Dewandel, B., Lanini, S., Hakoun, V., Caballero, Y. & Maréchal, J.-C. (2021) Artificial aquifer recharge and pumping: transient analytical solutions for hydraulic head and impact on streamflow rate based on the spatial superposition method. *Hydrogeology Journal*, 29(3), 1009–1026. Available from: https://doi.org/10.1007/s10040-020-02294-9

Dillon, P., Stuyfzand, P., Grischek, T., Lluria, M., Pyne, R.D.G., Jain, R.C. et al. (2019) Sixty years of global progress in managed aquifer recharge. *Hydrogeology Journal*, 27(1), 1–30. Available from: https://doi.org/10.1007/s10040-018-1841-z

Dione, A. (2012) Analyse de la durabilité des dynamiques d'extension des systèmes oasiens du Tafilalet, Sud-Est du Maroc.

El Khoumsi, W. (2017) Interactions hydriques palmier dattier-nappe phréatique et leurs impacts sur l'évolution des palmeraies: - cas des oasis de Tafilalet (Maroc). 203 pp, ISBN: 978-9981-801-81-3.

El Yadari, H., Chikhaoui, M., Naimi, M., Sabir, M. & Raclot, D. (2019) Techniques de conservation des eaux et des sols au Maroc: aperçu et perspectives. *Revue Marocaine Des Sciences Agronomiques et Vétérinaires*, 7, 343–355.

Faiz, M.E. & Ruf, T. (2010) An Introduction to the Khettara in Morocco: two contrasting cases. In: Schneier-Madanes, G. & Courel, M.-F. (Eds.) *Water and sustainability in arid regions: bridging the gap between physical and social sciences*. Netherlands, Dordrecht: Springer, pp. 151–163 https://doi.org/10.1007/978-90-481-2776-4_10

Finnemore, E.J. (1995) A program to calculate ground-water mound heights. *Groundwater*, 33, 139–143. Available from: https://doi.org/10.1111/j.1745-6584.1995.tb00269.x

Gee, G.W. & Hillel, D. (1988) Groundwater recharge in arid regions: review and critique of estimation methods. *Hydrological Processes*, 2(3), 255–266. Available from: https://doi.org/10.1002/hyp.3360020306

Godwin, I.A., Reba, M.L., Leslie, D.L., Adams, R.F. & Rigby, J.R. (2022) Feasibility of farm-scale infiltration galleries for managed aquifer recharge in an agricultural alluvial aquifer of Northeast Arkansas. *Agricultural Water Management*, 264, 107531. Available from: https://doi.org/10.1016/j.agwat.2022.107531

Guihéneuf, N., Boisson, A., Bour, O., Dewandel, B., Perrin, J., Dausse, A. et al. (2014) Groundwater flows in weathered crystalline rocks: impact of piezometric variations and depth-dependent fracture connectivity. *Journal of Hydrology*, 511, 320–334. Available from: https://doi.org/10.1016/j.jhydrol.2014.01.061

Hantush, M.S. (1967) Growth and decay of groundwater-mounds in response to uniform percolation. *Water Resources Research*, 3(1), 227–234. Available from: https://doi.org/10.1029/WR003i001p00227

Hashemi, H., Berndtsson, R., Kompani-Zare, M. & Persson, M. (2013) Natural vs. artificial groundwater recharge, quantification through inverse modeling. *Hydrology and Earth System Sciences*, 17(2), 637–650. Available from: https://doi.org/10.5194/hess-17-637-2013

Kendy, E., Gérard-Marchant, P., Walter, M.T., Zhang, Y., Liu, C. & Steenhuis, T.S. (2003) A soil-water-balance approach to

quantify groundwater recharge from irrigated cropland in the North China plain. *Hydrological Processes*, 17(10), 2011–2031. Available from: https://doi.org/10.1002/hyp.1240

Khardi, Y., Lacombe, G., Dewandel, B., Taky, A., Maréchal, J.-C., Hammani, A., et al. (2024) Managed groundwater recharge at the farm scale in pre-Saharan Morocco. In: *Proceedings of IAHS. Presented at the IAHS2022 – Hydrological sciences in the Anthropocene - IAHS Scientific Assembly 2022, Montpellier, France, 29 May–3 June 2022, Copernicus GmbH*, pp. 47–52. Available from: https://doi.org/10.5194/piahs-385-47-2024

Khardi, Y., Lacombe, G., Kuper, M., Taky, A., Bouarfa, S. & Hammani, A. (2023) Pomper ou disparaître: le dilemme du renforcement des khettaras par le pompage solaire dans les oasis du Maroc. *Cahiers Agricultures*, 32, 1. Available from: https://doi.org/10.1051/cagri/2022030

Koutous, A., Lacombe, G. & Hammani, A. (2023) Les "notfias" du Maroc: Une technique ancestrale de collecte et stockage des eaux pluviales. *Techniques Sciences Méthodes*, 7/8, 87–95. Available from: https://doi.org/10.36904/tsm/202307087

Lachassagne, P., Dewandel, B. & Wyns, R. (2021) Review: hydrogeology of weathered crystalline/hard-rock aquifers—guidelines for the operational survey and management of their groundwater resources. *Hydrogeology Journal*, 29(8), 2561–2594. Available from: https://doi.org/10.1007/s10040-021-02339-7

Lightfoot, D.R. (1996) Moroccan khettara: traditional irrigation and progressive desiccation. *Geoforum*, 27(2), 261–273. Available from: https://doi.org/10.1016/0016-7185(96)00008-5

Maréchal, J.C., Dewandel, B., Ahmed, S., Galeazzi, L. & Zaidi, F.K. (2006) Combined estimation of specific yield and natural recharge in a semi-arid groundwater basin with irrigated agriculture. *Journal of Hydrology*, 329(1-2), 281–293. Available from: https://doi.org/10.1016/j.jhydrol.2006.02.022

Msume, A.P., Mwale, F.D. & Castelli, G. (2022) Inventory and drivers of the adoption of flood-based farming systems in south-eastern Africa: insights from Malawi*. *Irrigation and Drainage*, 71(2), 521–533. Available from: https://doi.org/10.1002/ird.2664

ORMVA-Tf. (1987) Caractérisation et cartographie des sols du périmètre Goulmima-Tinjdad province d'Errachidia. Office régional de mise en valeur agricole du Tafilalet (ORMVA-Tf).

Prinz, D. (1996) Water harvesting – past and future. In: Pereira, L.S., Feddes, R.A., Gilley, J.R. & Lesaffre, B. (Eds.) *Sustainability of irrigated agriculture*. Proceedings, NATO Advanced Research Workshop, Vimeiro, 21-26.03, Balkema, Rotterdam, 135–144.

Sabir, M., Roose, E. & Al Karkouri, J. (2010) Les Techniques Traditionnelles de Gestion de l'eau, de La Biomasse et de La Fertilité Des Sols. In: IRD Editions. (Ed.) *Gestion durable des Eaux et des sols au Maroc: valorisation des techniques Traditionnelles Méditerranéennes*. Marseille: France, pp. 117–193. https://doi.org/10.4000/books.irdeditions.327

Sabri, A., Bouaziz, A., Hammani, A., Kuper, M., Douaik, A. & Badraoui, M. (2017) Effet de l'irrigation déficitaire contrôlée Sur la croissance et le développement foliaire du palmier dattier (*Phoenix dactylifera* L.). *Cahiers Agricultures*, 26(5), 55005. Available from: https://doi.org/10.1051/cagri/2017033

Sedra, M.H. (2003) Le palmier dattier base de la mise en valeur des oasis au Maroc: techniques phoenicicoles et création d'oasis, [WWW document]. INRA. https://www.inra.org.ma/sites/default/files/publications/ouvrages/palmierdattier.pdf (accessed 2.1.23), 265 pp, ISBN: 9981-1994-3-5.

Soni, P., Dashora, Y., Maheshwari, B., Dillon, P., Singh, P. & Kumar, A. (2020) Managed aquifer recharge at a farm level: evaluating the performance of direct well recharge structures. *Water*, 12(4), 1069. Available from: https://doi.org/10.3390/w12041069

Wang, B., Jin, M., Nimmo, J.R., Yang, L. & Wang, W. (2008) Estimating groundwater recharge in Hebei plain, China under varying land use practices using tritium and bromide tracers. *Journal of Hydrology*, 356(1-2), 209–222. Available from: https://doi.org/10.1016/j.jhydrol.2008.04.011

Warner, J., Molden, D., Chehata, M. & Sunada, D.K. (1989) Mathematical analysis of artificial recharge from basins1. *JAWRA Journal of the American Water Resources Association*, 25(2), 401–411. Available from: https://doi.org/10.1111/J.1752-1688.1989.TB03077.X

Water Resources Division. (1977) Ressources en eau Du MAROC Tome III: Hydrogéologie Bassin versant [WWW document]. Scribd. https://fr.scribd.com/document/494028246/Ressources-en-Eau-Du-MAROC-Tome-III (last access: 4 May 2022).

Wuilleumier, A. & Seguin, J.J. (2008) Réalimentation artificielle des aquifères en France, Une synthèse. BRGM/RP-55063-FR. Étude réalisée dans le cadre des projets de Service public du BRGM, 120.

Xu, C.-Y. & Chen, D. (2005) Comparison of seven models for estimation of evapotranspiration and groundwater recharge using lysimeter measurement data in Germany. *Hydrological Processes*, 19(18), 3717–3734. Available from: https://doi.org/10.1002/hyp.5853

Zhu, C. (2000) Estimate of recharge from radiocarbon dating of groundwater and numerical flow and transport modeling. *Water Resources Research*, 36(9), 2607–2620. Available from: https://doi.org/10.1029/2000WR900172

Zomorodi, K. (2012) Simplified solution for groundwater mounding under round stormwater infiltration facilities. In: *World Environmental and Water Resources Congress 2009*, pp. 1–17. Available from: https://doi.org/10.1061/41036(342)152

How to cite this article: Khardi, Y., Lacombe, G., Dewandel, B., Hammani, A., Taky, A. & Bouarfa, S. (2024) Conjunctive use of floodwater harvesting for managed aquifer recharge and irrigation on a date farm in Morocco. *Irrigation and Drainage*, 1–13. Available from: https://doi.org/10.1002/ird.2967

APPENDIX A

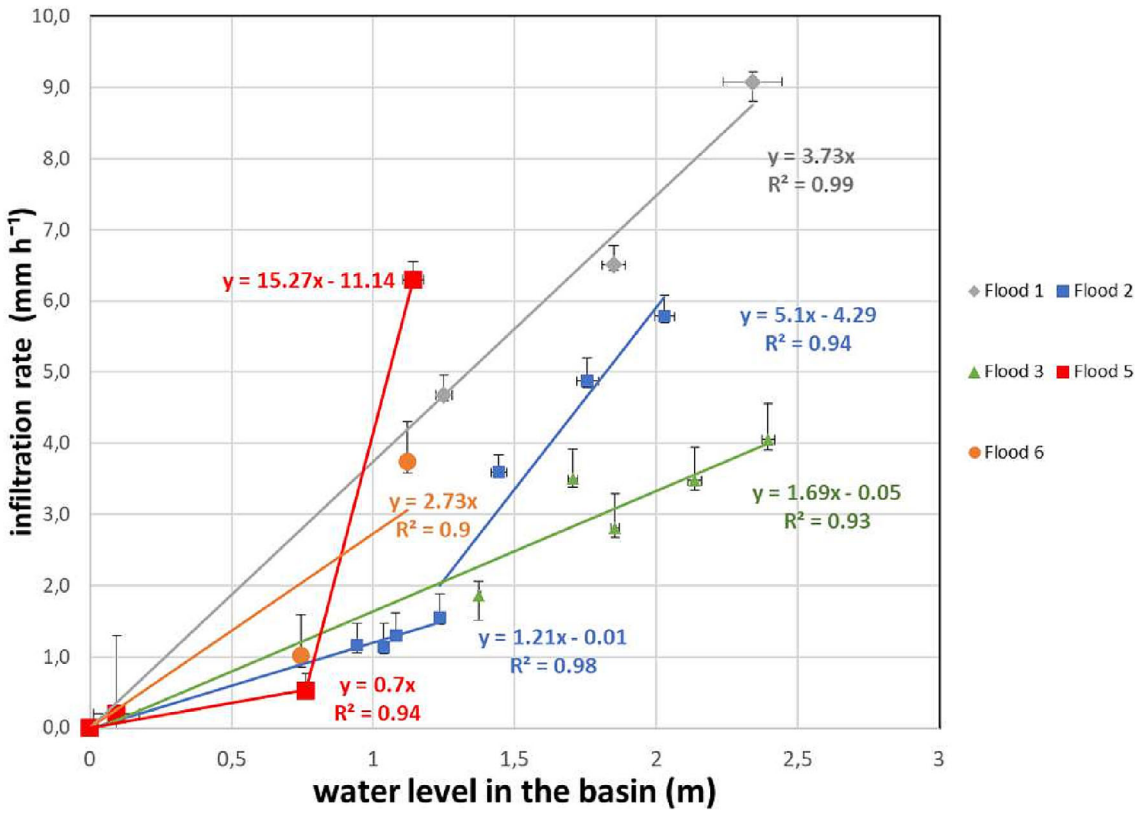

FIGURE A1 The uncertainties related to the infiltration rates are represented by vertical bars. The horizontal bars represent the range of water levels selected to calculate infiltration.